

Reports

Algal Fossils from a Late Precambrian, Hypersaline Lagoon

Abstract. *Organically preserved algal microfossils from the Ringwood evaporite deposit in the Gillen Member of the Bitter Springs Formation (late Precambrian of central Australia) are of small size, low diversity, and probable prokaryotic affinities. These rather primitive characteristics appear to reflect the stressful conditions that prevailed in a periodically stagnant, hypersaline lagoon. This assemblage (especially in comparison with the much more diverse assemblages preserved in the Loves Creek Member of the same formation) illustrates the potential utility of Proterozoic microbiotas for basin analysis and local stratigraphic correlation and demonstrates the need to base evolutionary considerations and Precambrian intercontinental biostratigraphy on biotas that inhabited less restricted environments.*

Among the major goals in Precambrian paleontology are (i) establishment of local and intercontinental systems of biostratigraphy, (ii) determination of the time of origin of eukaryotic organisms, and (iii) development of the ability to use Proterozoic microbiotas for paleoenvironmental interpretation and basin analysis. A recently discovered microflora from the Gillen Member of the Bitter Springs Formation has bearing on each of these objectives. Although significant in itself, this assemblage becomes particularly important when compared with the well-known, considerably more diverse, and evidently more advanced biotas of the immediately overlying Loves Creek Member (1) of the same formation.

The Bitter Springs Formation is late Precambrian in age [740 ± 30 to 1076 ± 50 million years old (2, 3)] and crops out along the northern margin of the Amadeus Basin in central Australia (4). It is about 1000 m thick and consists of two members, the Loves Creek Member (upper) and the Gillen Member (lower). The fossils here described are from the Ringwood evaporite deposit, which occurs within the Gillen Member at a location about 100 km east of Alice Springs. They are preserved in cherty areas of silicified dolomite sampled from the 170.7-m level of a Bureau of Mineral Resources (Canberra) drill core (BMR Alice Springs No. 3, registration No. 1002; housed in BMR Core and Cuttings Laboratory).

The fossiliferous rocks are from the lower part of a marine evaporite sequence (5) of the classical barred-basin type (6). The upper part of the sequence is characterized by gypsum, gypsiferous dolomite with rare laminae of arkosic

silt, and clayey dolomite. The lower part contains very fine-grained bituminous dolomite, dolomite breccia cemented by coarsely crystalline anhydrite, siliceous laminae and oolites, and disseminated pyrite. Partial silicification of the dolomite is common. The uniform, fine-grained nature of the dolomite laminae and lack of replacement textures suggest that the dolomite formed either by primary precipitation or by early diagenetic alteration of calcite or aragonite. Much of the silica is secondary although some appears to be primary, perhaps having formed contemporaneously with the dolomite as an opaline precipitate similar to that forming today in lakes associated with the Coorong Lagoon in South Australia (7).

Geologic data indicate that this sequence formed in a warm, restricted, hypersaline lagoon inside an offshore algal reef (5). This interpretation is supported by organic geochemical data obtained by McKirdy (8) on extracts from the bituminous dolomite (high naphthene concentration, depleted *n*-alkanes, pristane/*n*-C₁₇ and phytane/*n*-C₁₈ ratios ≥ 1, and an even-carbon-number predominance among C₂₀ to C₃₀ *n*-alkanes). The geochemical data further suggest extensive bacterial degradation of the algal material in these sediments (8, 9). McKirdy (8) concluded that these particular dolomites contain largely indigenous bitumen and are not significantly contaminated by migrated, postdepositional hydrocarbons.

The Gillen Member assemblage is dominated by spheroidal to ellipsoidal bundles of densely interwoven tubules (Fig. 1, A to E) interpreted as the sheaths of filamentous blue-green algae. The sheaths are cylindrical, unbranched,

smooth, and unlamellated. They may be darkly pigmented (Fig. 1F) and apparently were quite flexible (Fig. 1E). They range in diameter from 2 to 10 μm (average 4 μm) and appear to be at least 25 times longer than wide. Sheath thickness ranges from 0.2 to 2.6 μm (average about 0.9 μm) and commonly is about one-fourth to one-third of the sheath diameter (Fig. 1F). In rare cases, they contain thin, single strands of dark particles (up to 0.5 μm across) which are interpreted as degraded cellular trichomes (Fig. 1, G and H). The bundles of intertwined sheaths and filaments (here referred to as algal balls; for example, see Fig. 1, A to C) are commonly 100 to 200 μm across, at least partially silicified, and often bordered by rims (about 25 μm thick) of finely granular dolomite (Fig. 1D). The algal balls resemble oolites in gross morphology and tend to be concentrated in discrete layers separated by continuous organic laminae (Fig. 1A). In many of the algal balls, the organic matter is severely degraded, such that fossils are preserved at the periphery only, in the center only, or not at all (Fig. 1, B and C). In size, morphology, and entangled growth form, these fossils resemble several genera of modern nostocalean blue-green algae [for example, *Symploca* and *Plectonema* (10)]. They may be related to the somewhat thinner, interwoven tubules that form mats in *Stratificera*-type stromatolites from the Riphean of the Soviet Union (11) and possibly to some of the Phanerozoic, oncolite-forming masses of calcified algal sheaths assigned to the genus *Girvanella* (12).

Unicellular fossils are rare in this assemblage, but two basic types have been recognized. Relatively large cells (12 to 14 μm in diameter) occur singly and in groups of up to four individuals within the algal balls (Fig. 1, I and K). They have walls up to 1 μm thick that often are irregularly degraded to form granular and patchy surface textures (Fig. 1I). Smaller unicells (3.7 to 7.5 μm in diameter; average 5 μm) occur singly and in enveloped, "gloeocapsoid" clusters of a few to several tens of individuals (Fig. 1J). These smaller cells generally are interspersed between the algal balls; some are present within the continuous organic laminae. The spheroidal fossils in this assemblage are probably of prokaryotic affinities, as they are relatively small, morphologically simple, and lack internal structures or trilete markings that might be suggestive of eukaryotic organization (13, 14). Some contain irregular masses of material interpreted as degraded cytoplasmic residues (Fig. 1, J and K); these residues are highly vari-

able in size and shape and lack the structural integrity, sharply defined boundaries, and other characteristics [see table 1 of (14)] that typify the organelle-like bodies in unicellular eukaryotes of the Loves Creek Member. The larger cells resemble coccoid microfossils reported from several other Proterozoic localities (1, 11, 15-17), while the smaller cells resemble morphological variants of *Eoentophysalis belcherensis* Hofmann from the middle Proterozoic of Canada and Australia (16, 17).

The spheroidal shapes of the algal balls and the uniform thickness of their individual carbonate rims suggest that these masses of filaments grew unattached to the substrate. Their concentration in discrete layers suggests that they bloomed periodically or were washed into the lagoonal setting episodically from adjacent localities. The continuous organic laminae between the layers of algal

balls (Fig. 1A) are generally amorphous, but their shapes, diffuse crests (Fig. 1L), and occasional inclusion of small unicells are features similar to those of laminae formed from degraded colonies of *E. belcherensis* in the 1500-million-year-old Balbirini Dolomite of northern Australia (17). It is possible, therefore, that these continuous laminae are remnants of *E. belcherensis* mats that were almost completely degraded by bacterial activity during highly stagnant periods. This would be consistent with the geochemical and geological data, the comparison of the smaller unicells with *E. belcherensis*, the spatial distribution of small unicells between algal balls, and the overall low percentage (less than 10 percent) of unicells in this deposit.

In its limited diversity and apparently prokaryotic nature, the Gillen Member assemblage contrasts markedly with the biotas reported from the Loves Creek

Member (1). These contrasts appear to reflect different environments of growth: the restricted, periodically stagnant, hypersaline conditions during deposition of the Ringwood evaporite deposit as compared with the more open, shallow marine depositional environment of the microfossiliferous units in the Loves Creek Member [gypsum, anhydrite, and pseudomorphs after evaporites are rare or absent in this latter member (2)]. Indeed, similar biological differences are well known in modern algal populations that live in various subenvironments of the intertidal to supratidal zone (18).

The low diversity and prokaryotic nature of the Gillen Member biota could be interpreted (incorrectly) as indicating a lack of eukaryotes and a paucity of species during this period of earth history, were it not for the fact that assemblages such as those of the Loves Creek Member are already documented. Instead,

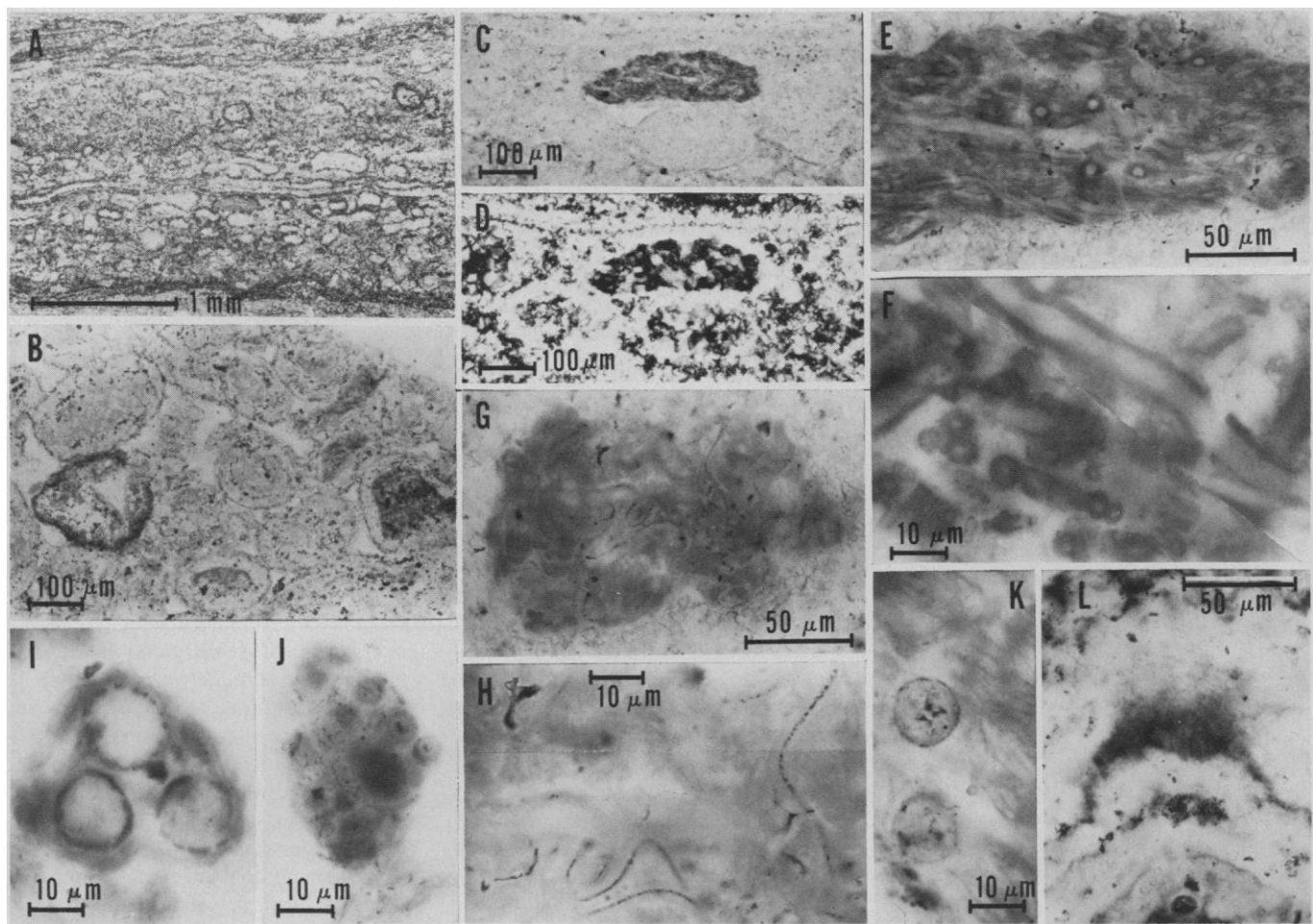


Fig. 1. Optical photomicrographs of organically preserved fossils in thin sections of silicified carbonate from the Gillen Member of the Bitter Springs Formation. (A) Overview showing typical layers of algal balls separated by continuous, dark organic laminae; (B) algal balls with microfossils (dark areas) preserved at peripheries, centers, or not at all (pale spheroids); (C) algal ball composed of densely interwoven, tubular filaments (paler spheroids are unfossiliferous); (D) same field of view as in (C), photographed under crossed Nicol prisms to show carbonate rims around the algal balls [carbonate rims are also visible in (B)]; (E) higher-magnification view of the algal ball in (C), showing interwoven tubular filaments; (F) longitudinal sections and cross sections of interwoven filaments, illustrating their thickness and dark pigmentation; (G) algal ball showing degraded trichomes preserved in centers of some filaments; (H) higher-magnification view of (G), illustrating particulate nature of degraded trichomes; (I) three unicells preserved within an algal ball; (J) cluster of "gloeocapsoid" packets of unicells; (K) two unicells within a bundle of filaments; and (L) convex upward portion of an organic lamina, showing diffuse nature of the crest (crestal area contains minute unicells).

these features are almost certainly the result of environmentally stressful conditions that would have excluded contemporary eukaryotes as well as many types of cyanophytes.

This report has shown that geological, geochemical, and paleontological data can be used to interpret the paleoecology of at least some kinds of Proterozoic, fossiliferous deposits. It also demonstrates that microbiotas of Precambrian hypersaline environments, like those of their modern counterparts, have low species diversity, are dominated by prokaryotic organisms, and consequently should not be used for inferring the evolutionary status of the contemporary biosphere or for considerations of evolutionary trends, such as age-related changes in algal diversity and size distribution (19). Comparison of the Gillen Member and Loves Creek Member assemblages provides an excellent example of environmental control over the composition of Precambrian biotas. It suggests that the two assemblages, and others of their types, can be useful for local biostratigraphic correlation, for basin analysis, and for environmental interpretation.

DOROTHY Z. OEHLER

JOHN H. OEHLER

Exploration Research Division,
Continental Oil Company,
Ponca City, Oklahoma 74601

ALASTAIR J. STEWART
Bureau of Mineral Resources, Geology
and Geophysics, Canberra City,
A.C.T. 2601, Australia

References and Notes

- J. W. Schopf, *J. Paleontol.* **42**, 651 (1968); and J. M. Blacic, *ibid.* **45**, 925 (1971).
- M. R. Walter, *Spec. Pap. Palaeontol.* No. 11 (1972).
- R. W. Marjoribanks and L. P. Black, *J. Geol. Soc. Aust.* **21**, 291 (1974).
- A. T. Wells, D. J. Forman, L. C. Ranford, P. J. Cook, *Bull. Bur. Miner. Resour. Geol. Geophys. Aust.* **100** (1970).
- A. J. Stewart, *Rec. Bur. Miner. Resour. Geol. Geophys. Aust.* **1974/145** (1974); *Sedimentology*, **26**, 33 (1979).
- C. Oehsenius, *Die Bildung der Steinsalzlager und ihrer Mutterlaugensalze* (Pfeffer, Halle, 1877).
- M. N. A. Peterson and C. C. von der Borch, *Science* **149**, 1501 (1965).
- D. M. McKirdy, thesis, Australian National University (1977).
- H. Dembicki, Jr., W. G. Meinschein, D. E. Hattin, *Geochim. Cosmochim. Acta* **40**, 203 (1976).
- T. V. Desikachary, *Cyanophyta* (Indian Council of Agricultural Research, New Delhi, 1959), pp. 58-60, 68, 334-340, and 434-441.
- J. W. Schopf, C. V. Mendelson, A. V. Nyberg, T. A. Dolnik, I. N. Krylov, B. B. Nazarov, Yu. K. Sovietov, M. S. Yakshin, *Precambrian Res.* **4**, 269 (1977).
- R. Riding, *Palaeontology* **20**, 33 (1977).
- D. Z. Oehler, *J. Paleontol.* **50**, 90 (1976); J. H. Oehler, D. Z. Oehler, M. D. Muir, *Origins Life* **7**, 259 (1976); J. W. Schopf and D. Z. Oehler, *Science* **193**, 47 (1976).
- D. Z. Oehler, *J. Paleontol.* **51**, 885 (1977).
- M. D. Muir, *Alcheringa* **1**, 143 (1976); J. H. Oehler, *ibid.* **1**, 315 (1977).
- H. J. Hofmann, *J. Paleontol.* **50**, 1040 (1976).
- D. Z. Oehler, *Alcheringa* **2**, 269 (1978).
- B. W. Logan, P. Hoffman, C. D. Gebelein, *Am. Assoc. Pet. Geol. Mem.* **22**, 140 (1974); P. Hoffman, in *Stromatolites*, M. R. Walter, Ed. (Elsevier, Amsterdam, 1976), pp. 261-271; P. E. Playford and A. E. Cockbain, *ibid.*, pp. 389-411.
- J. W. Schopf, *Precambrian Res.* **5**, 143 (1977).
- Published with permission of the director, Bureau of Mineral Resources, Geology and Geophysics, Canberra, and approval of the manager, Exploration Research Division, Continental Oil Company, Ponca City.

17 April 1979

Isotope Selectivity of Infrared Laser-Driven Unimolecular Dissociation of a Volatile Uranyl Compound

Abstract. *Isotope-selective photodissociation of the volatile complex uranyl hexafluoroacetylacetonate · tetrahydrofuran [UO₂(hfacac)₂ · THF] has been achieved with both a continuous-wave and a pulsed carbon dioxide laser. The photodissociation was carried out in a low-density molecular beam under collisionless conditions. Transitions of the laser are in resonance with the asymmetric O-U-O stretch of the uranyl moiety, a vibrational mode whose frequency is sensitive to the masses of the uranium and oxygen isotopes. Unimolecular dissociation is observed mass spectrometrically at an extremely low energy fluence, with no evidence of an energy fluence or intensity threshold. The dissociation yield increases nearly linearly with increasing energy fluence. At constant fluence the dissociation yield is independent of contact time between the radiation field and the molecule, indicating that the decomposition is driven by laser energy fluence and not laser intensity. The oxygen and uranium isotope selectivities measured in these experiments are nearly those predicted by the ratio of the linear absorption cross sections for the respective isotopes. Thus, essentially complete selectivity is observed for oxygen isotopes, while a selectivity of only about 1.25 is measured for the uranium isotopes. A model presented to describe these results is based on rapid intramolecular vibrational energy flow from the pumped mode into a limited number of closely coupled modes.*

We report here the uranium and oxygen isotope selective unimolecular dissociation of a volatile uranium-bearing complex, uranyl hexafluoroacetylacetonate · tetrahydrofuran [UO₂(hfacac)₂ · THF], using either a pulsed or a continuous-wave (CW) CO₂ laser. Energy is deposited in this molecule by excitation of the O-U-O asymmetric stretch of the uranyl moiety. This vibrational mode is in resonance with several of the 10.6-μm transitions of the CO₂ laser and is spectroscopically selective for the isotopes of both uranium and oxygen. The absorption spectrum of this vibrational mode for an oxygen-18-enriched sample is indicated in Fig. 1. The 17-cm⁻¹ isotope shift between U¹⁶O₂ and U¹⁸O₂-bearing species is greater than the width of the absorption band and results in spectrally resolved infrared (IR) bands for the oxygen isotopes. The uranium isotope shift, however, is only 0.7 cm⁻¹, and although either uranium isotope can be preferentially excited depending on the laser transition used, the IR absorption features are not spectrally resolved. Thus we can examine, in the same molecule, the effects of overlapping and nonoverlapping IR absorption bands on the isotope selectivity.

Previously we reported (1) the unimolecular decomposition of this molecule with a pulsed CO₂ laser. The results

described here also demonstrate that a CW IR laser can induce the unimolecular dissociation of such molecules. Recently the unimolecular decomposition of ions with a CW CO₂ laser was reported (2). Multiple photon excitation of uranyl molecules differs from excitation of smaller molecules, for which the anharmonicity barrier is a critical factor. For this molecule the multiple photon process is postulated to be repeated excitation of the 0-1 vibrational transition of the O-U-O asymmetric stretch. This mode relaxes rapidly by an intramolecular vibrational energy transfer into a small subset of strongly coupled modes, leaving the asymmetric stretch in its ground vibrational state so that subsequent photons can be absorbed. The vibrational relaxation time is required to be shorter than 10⁻⁹ second so that at laser intensities of only a fraction of a megawatt per square centimeter, the few CO₂ laser photons necessary to overcome the barrier to dissociation can be absorbed during the laser contact time with the molecule. This model for multiple photon excitation and the implication for IR laser-induced chemistry in large molecules have been described (1). The factors concerning the isotope selectivity of this process are described in this report.

Experimental. The molecule UO₂-